

## Enhanced Extreme Ultraviolet Lithography Mask Inspection Contrast Using Fabry-Perot Type Antireflective Coating

Hsu-Chun CHENG, Hsuen-Li CHEN<sup>1,\*</sup>, Tsung-Shine KO<sup>2</sup>, Lee-Jene LAI<sup>3</sup>, Fu-Hsiang KO and Tieh-Chi CHU<sup>2</sup>

National Nano Device Lab., Hsinchu, Taiwan, R. O. C.

<sup>1</sup>Department of Materials Science and Engineering, National Taiwan University, Taiwan, R. O. C.

<sup>2</sup>National Tsing Hua University, Hsinchu, Taiwan, R. O. C.

<sup>3</sup>National Synchrotron Radiation Research Center, Hsinchu, Taiwan, R. O. C.

(Received October 31, 2003; revised January 9, 2004; accepted January 28, 2004; published June 29, 2004)

In this paper, we describe two strategies for solving the low-contrast problem during extreme ultraviolet lithography (EUVL) mask inspection processes. One is the use of single-layer antireflective coating (ARC), and the other is the use of Fabry-Perot-type ARC. The materials of ARC are the same as those of buffer layers, such as SiO<sub>2</sub> and Si<sub>3</sub>N<sub>4</sub>, which are easy to fabricate. Contrast can be increased up to >95% by adding ARC. For both absorbers, Single-layer Si<sub>3</sub>N<sub>4</sub> ARC and Si<sub>3</sub>N<sub>4</sub>-based Fabry-Perot-type ARC show better performances than SiO<sub>2</sub> ARC. Both types of ARC maintain a high contrast at 40% with a large thickness variation even until ±40%. Moreover, the top absorber in Fabry-Perot-type ARC has good conductivity that can eliminate electrical distortion, which is caused by electron charging during e-beam direct writing. The Fabry-Perot-type ARC structure has better contrast and thickness variation tolerance than the single-layer ARC structure. The film materials in Fabry-Perot structure can also be used for various absorber and dielectric materials. [DOI: 10.1143/JJAP.43.3703]

KEYWORDS: extreme ultraviolet lithography, absorber, buffer layer, antireflective coatings, Fabry-Perot

### 1. Introduction

Extreme ultraviolet lithography is one of the leading candidates for patterning semiconductor devices for sub-50 nm generations.<sup>1)</sup> In recent years, a wide range of absorber and buffer layer materials have been evaluated as potential absorber materials for extreme ultraviolet lithography (EUVL) mask applications.<sup>2)</sup> TaN and Cr are the leading choices for absorber materials. Si<sub>3</sub>N<sub>4</sub> and SiO<sub>2</sub> have been widely used as buffer layers.<sup>3)</sup>

TaN and Cr exhibit characteristics as absorbers at the EUV wavelength (13.4 nm) but have a high reflectance at the deep ultraviolet (DUV) inspection wavelength (257 nm or 365 nm). The high reflectance from the absorber stack decreases the contrast between multilayer stacks during inspection. Therefore, increasing the inspection contrast by decreasing reflectance from the absorber stack at the inspection wavelength is essential.

Traditionally, a mask is fabricated by electron beam direct writing. Electrons intrinsically accumulate on the incident substrate that causing following electron deflection. The problem will become more serious in the current EUVL mask fabrication than in past fabrication when the feature size was less than 200 nm. To avoid pattern distortion, the substrate should have good conductivity. General single-layer antireflective coatings (ARCs), which are dielectric materials with poor conductivity, are not suitable substrates in e-beam direct writing.

In this paper, we will demonstrate two simple ARC structures the use of which enables absorber stacks to meet the exposure and inspection requirements simultaneously. The thickness of ARC was optimized to minimize the reflectance at 257 nm. We also considered solving the charging effect caused by electron accumulation using Fabry-Perot-type ARC. The total thickness of the absorber stacks were maintained below 150 nm to meet the stack height requirement thus preventing the geometric shadow effect.

Table I. Optical constant of EUVL mask materials at 257 nm wavelength.

	n	k
Si	1.8411	2.8374
Mo	1.7170	3.7458
SiO <sub>2</sub>	1.5041	0
Si <sub>3</sub> N <sub>4</sub>	2.2475	0.0023
TaN	2.4967	1.5257
Cr	1.3776	1.9878

$\lambda = 257 \text{ nm}$

### 2. Simulation

For all calculations, we used a commercial thin-film design program (SCI Film Wizard). The optical constants of molybdenum (Mo), silicon (Si), tantalum nitride (TaN), chrome (Cr), silicon dioxide (SiO<sub>2</sub>), and silicon nitride (Si<sub>3</sub>N<sub>4</sub>) at EUV and DUV wavelengths from the Henke table<sup>4)</sup> were imported to this program. Table I lists the optical constants of EUVL mask materials in the 257-nm-inspection-wavelength regions.

For characterizing reflectance behavior, we assume multi-layer (ML) coatings consisting of 40-layer pairs of Mo and Si with layer thicknesses of 2.8 and 4.1 nm, respectively.<sup>5)</sup> The Mo/Si ML coatings were deposited on a low-thermal-expansion material (LTEM) substrate and then covered with buffers and absorbers by the PVD method. We assume that the thickness of buffer was approximately 60 nm to meet the requirement of the focused ion beam (FIB) repair stage. The thickness of the absorber was 60 nm to achieve a low reflectance (<0.1%) at an exposure wavelength with and without ARC.

### 3. Results and Discussion

To simplify discussion, we obtain the same reflectance from ML stacks at the repair and final stages by calculating reflectance from the ML stack with different buffer layer thicknesses. As shown in Fig. 1, the reflectance from the ML

\*E-mail address: hlchen@ndl.gov.tw

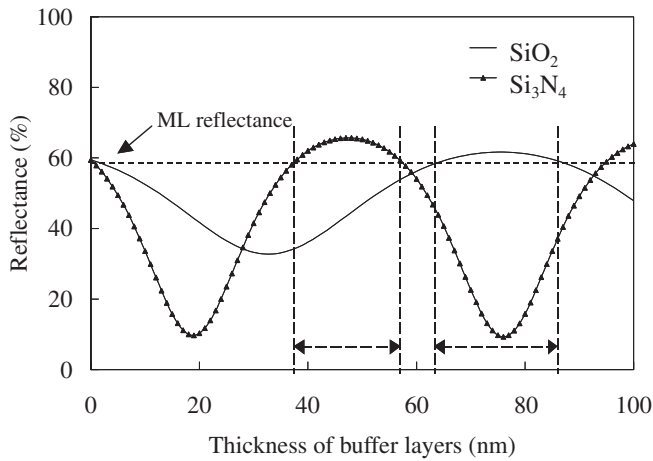


Fig. 1. Reflectance from ML mirror and different thicknesses of buffer layers.

stack is about 60% at 257 nm. Here, we design the ARC to increase contrast by decreasing the reflectance from the absorber stacks. Therefore, the reflectance from the ML stack with a buffer should be higher or equal to 60%. According to this viewpoint, the thickness of ARC should be chosen as 38 to 58 nm for  $\text{Si}_3\text{N}_4$ , and 64 to 85 nm for  $\text{SiO}_2$ . However, through the considerations of stack thickness and FIB repair requirement, an etching selectivity of the absorber to the buffer is about 1, a buffer layer thickness of about 60 nm are necessary. The reflectance at such buffer layer thickness is almost the same as the final-stage buffer layer thickness. Hence, the following results and discussions focus only on the final-stage inspection, in which the reflectance is about 60%.

### 3.1 Single-layer ARC

Figure 2 shows the diagram of the single-layer ARC structure. By common consideration, we chose only  $\text{SiO}_2$

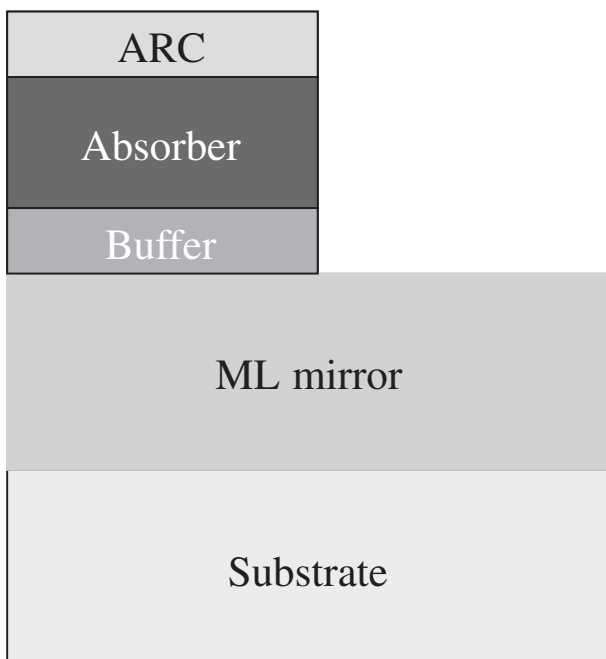


Fig. 2. Diagram of single-layer antireflective coating structure.

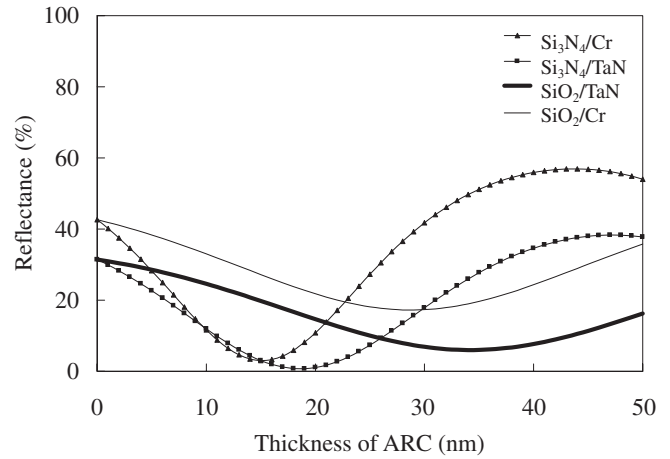


Fig. 3. Reflectance from absorber stacks with single-layer ARC at 257 nm inspection wavelength.

and  $\text{Si}_3\text{N}_4$  in our simulations. Of course, other materials such as  $\text{SiON}$ ,  $\text{Ta}_2\text{O}_5$ , and  $\text{Cr}_2\text{O}_3$  could also be used for ARC. Here, we selected the same ARC material with a buffer to simplify the blank mask fabrication process. Figure 3 shows the reflectance from absorber stacks with different ARC thicknesses. As shown in the figure, the reflectance from the absorber stack become minimum after capping  $\text{Si}_3\text{N}_4$  and  $\text{SiO}_2$  of different thicknesses. The reflectance from thin  $\text{Si}_3\text{N}_4$ -ARC-capped absorbers is lower than that from thick  $\text{SiO}_2$ -ARC-capped ones. By adding <20 nm  $\text{Si}_3\text{N}_4$ , the reflectance from the Cr absorber could be decreased to 3% and that from the TaN absorber to 1%. It is clearly seen that  $\text{Si}_3\text{N}_4$  has better performance than  $\text{SiO}_2$  in terms of reflectance and total thickness.

From previous discussions, the optimum thickness of single-layer ARC was determined. However, it is difficult to produce perfect ARC in actual situations. What of the exact thickness could not be deposited, and a slight inaccuracy existed. The variation of single-layer ARC thickness causes contrast degradation under most conditions but still satisfies the inspection contrast threshold, which should be at least 40%. However, in the worst case, for the  $\text{SiO}_2$ -capped Cr absorber, the contrast is still higher than 40% when the ARC thickness varied from  $\pm 40\%$  ( $\pm 11.6$  nm), as shown in Fig. 4. In the best case, for the  $\text{Si}_3\text{N}_4$ -capped TaN absorber, the contrast is still higher than 40% when the ARC thickness varied from  $\pm 80\%$  ( $\pm 15.2$  nm). By controlling  $\text{Si}_3\text{N}_4$  ARC thickness well, the contrast can be from TaN and Cr raised to 97.5% and 90%, respectively. These should be acceptable values for all existing equipment.

Both  $\text{Si}_3\text{N}_4$  and  $\text{SiO}_2$  could be used to upgrade the contrast even for TaN or Cr absorbers. From the optical viewpoint, they are almost the flawless materials. However, there is a fatal drawback, that is, conductivity. To generate perfect antireflective structures, the idea of Fabry-Perot-type ARC was proposed.

### 3.2 Fabry-Perot-type ARC

Figure 5 shows a Fabry-Perot-type ARC structure, which comprise a dielectric layer and a thin absorber layer. In general, the mask layer should have good electrical conductivity for e-beam writing in order to prevent writing

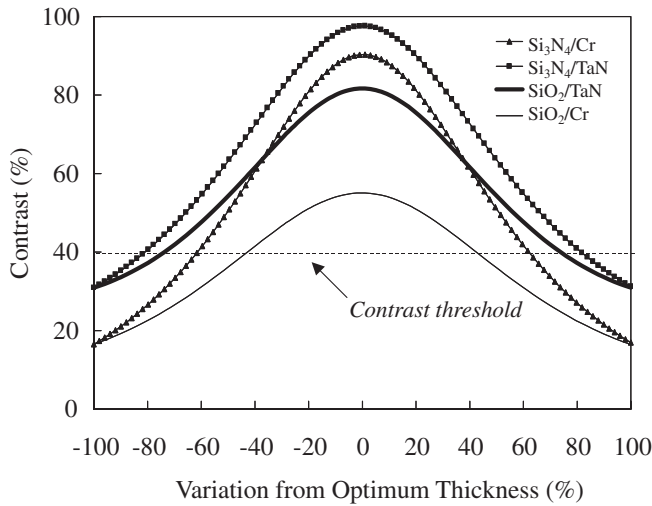


Fig. 4. Thickness variation tolerance of single-layer ARC.

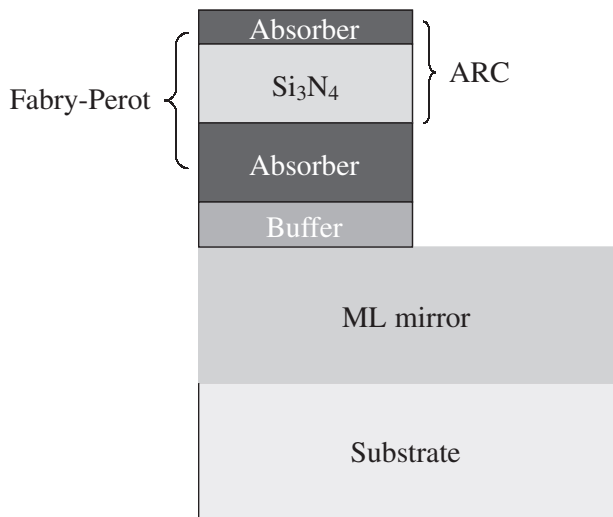


Fig. 5. Diagram of a Fabry-Perot-type antireflective coating structure.

errors due to charging effects. In the Fabry-Perot structure, the top absorber layer can prevent charge accumulation during e-beam writing. By controlling the thickness of the dielectric layer, we can easily tune the minimum reflection region to the desired inspection wavelength. The reflectances at 257 nm are shown in Fig. 6. We fixed the thickness of the top absorber layer at several nm and change the thickness of the bottom dielectric layer to evaluate reflectance from the stack. The total absorber thickness in the stack was fixed at 60 nm and it is easy to achieve both low EUV reflectance and high DUV contrast by controlling the Si<sub>3</sub>N<sub>4</sub> or SiO<sub>2</sub> thickness well. As shown in Fig., SiO<sub>2</sub> has the same performance as Si<sub>3</sub>N<sub>4</sub> in terms of reflectance, but is thicker. Reflectance decreases to <1% in all cases when the thicknesses of Si<sub>3</sub>N<sub>4</sub> and SiO<sub>2</sub> were about 20 nm and 30 nm, respectively. All contrasts are higher than 95%.

Similarly, we focus on the contrast decrease caused by varying ARC thickness. Figure 7 shows the relationship between the thickness of Si<sub>3</sub>N<sub>4</sub>-based Fabry-Perot-type ARC and contrast. Both the top absorber and bottom dielectric layers of Fabry-Perot-type ARC show good thickness variation tolerance.

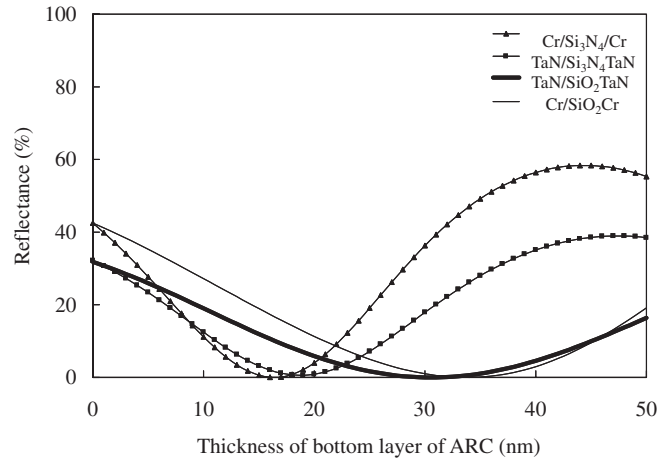


Fig. 6. Reflectance from absorber stacks with a Fabry-Perot-type ARC at 257 nm inspection wavelength.

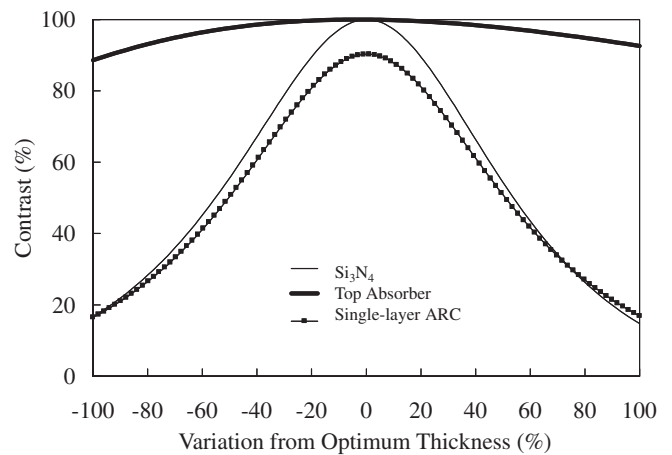


Fig. 7. Comparison of contrast and thickness tolerance between single-layer and Fabry-Perot-type ARCs.

### 3.3 Comparisons of single-layer ARC and Fabry-Perot-type ARC

As shown in Fig. 7, Cr is the absorber and Si<sub>3</sub>N<sub>4</sub> is the single-layer ARC. By comparing the thickness tolerance and performance of these two ARC structures, Fabry-Perot-type ARC shows better performance than single-layer ARC. As summarized in Table II, the contrasts without adding ARC were 30.9% and 16.5% from TaN and Cr absorbers, respectively. It is difficult to recognize pattern defects using the inspection equipment at this low contrast level. After capping a SiO<sub>2</sub> single-layer ARC, the contrasts were raised to 81.7% and 55.1%. These are acceptable inspection thresholds but not sufficiently good. Thus, we raised the

Table II. Contrasts (%) of traditional EUVL mask with/without ARC at 257 nm wavelength.

	Without ARC	With ARC			
		Single-layer		F-T type	
		SiO <sub>2</sub>	Si <sub>3</sub> N <sub>4</sub>	SiO <sub>2</sub>	Si <sub>3</sub> N <sub>4</sub>
TaN	30.9	81.7	97.5	>99	98
Cr	16.5	55.1	90.3	>99	>99

Table III. Total thickness (nanometer) of absorber stacks with/without ARC.

	Without ARC	With ARC			
		Single-layer		F-T type	
		SiO <sub>2</sub>	Si <sub>3</sub> N <sub>4</sub>	SiO <sub>2</sub>	Si <sub>3</sub> N <sub>4</sub>
TaN	120	34/120	19/120	31/120	19/120
Cr	120	29/120	15/120	34/120	16/120

contrasts to 97.5% and 90.3% by capping Si<sub>3</sub>N<sub>4</sub> single-layer ARC. These results seem to be better than those of SiO<sub>2</sub>-capped ones.

Furthermore, as shown in Table III, the total thickness of the SiO<sub>2</sub>-capped absorber stacks were too large to conform to the rule that the thickness should as small as possible. On the other hand, the Si<sub>3</sub>N<sub>4</sub>-capped absorber stack fulfilled the requirement.

Similarly, the contrasts could be raised to more than 95% by adding Fabry-Perot-type ARC in all situations. The thicknesses of stacks were almost the same as that for single-layer ARC that did not increase much. Si<sub>3</sub>N<sub>4</sub> performs better than SiO<sub>2</sub> in a comprehensive survey. Thickness variation tolerance was as large as that of the single-layer ones. In

addition, Fabry-Perot-type ARC has good conductivity to eliminate the charging effect during e-beam writing.

#### 4. Conclusions

Two types of ARC were demonstrated by simulation. Single-layer ARC has an acceptable contrast that meets equipment requirements. Fabry-Perot-type ARC not only shown excellent contrast but also good conductivity. It can eliminate the electron charging effect thereby preventing pattern distortion during mask fabrication and raising contrast during the inspection process simultaneously. Thinner Si<sub>3</sub>N<sub>4</sub> had a higher contrast than thicker SiO<sub>2</sub>. However, from the viewpoint of contrast and stack thickness that induce the geometric shadow effect, the Si<sub>3</sub>N<sub>4</sub> performed better than SiO<sub>2</sub> in both types ARC.

- 1) S. D. Hector: SPIE **4688** (2002) 134.
- 2) P. Y. Yan, G. Zhang, A. Ma and T. Liang: SPIE **4343** (2001) 409.
- 3) K. H. Smith, J. R. Wasson, P. J. S. Mangat, W. J. Dauksher and D. J. Resnick: J. Vac. Sci. & Technol. B **19** (2001) 2906.
- 4) B. L. Henke, E. M. Gullikson and J. C. Davis: At. Data & Nucl. Data Tables **54** (1993) 181.
- 5) S. D. Hector and P. Mangat: J. Vac. Sci. & Technol. B **19** (2001) 2612.